Preliminary results of PIV measurement past a stator wheel inside the VT-400 test turbine

Daniel Duda[1], *Vít* Horáček[1], *Marek* Klimko[1], *Petr* Milčák[3], *Václav* Uruba[1,2], *Vitalii* Yanovych[1,2] and *Pavel* Žitek[1*]

[1]Faculty of Mechanical Engineering, University of West Bohemia in Pilsen, Univerzitní 22, 306 14, Pilsen, Czech Republic
[2]Institute of Thermomechanics, Czech Academy of Sciences, Dolejškova 5, 180 00, Prague, Czech Republic
[3]Doosan Škoda Power, Tylova 16, 301 00, Pilsen, Czech Republic

Abstract. The feasibility study of Particle Image Velocimetry (PIV) measurements inside a test turbine at the University of West Bohemia. The current VT-400 turbine is not prepared for optical measurement with seeding particles, thus several technical issues had to be addressed until low-quality data were obtained only at low speed of 2000 RPM (rounds per minute). Even the low quality data are able to show the fluctuation anisotropy or the size of fluctuation structures, which are quantities not measurable by classical pressure methods.

1 Introduction

This year, 2022, we "celebrate" two centuries since phenomenological definition of turbines in 1822 [1] by Claude Burdin. The phenomenological definition is mentioned, because such type of machines is much elder, however, it has been constructed in a form of windmill (6th century, Persia), windpump or waterwheel (for powering watermill (3rd century BC, Byzantinum [2]) or waterpump (5th century BC, China [3])). Probably, it has to be much elder: although there is no any direct archeologic or written evidence, it seems, that Sumerians had to have this technology [4] as well.

Since 18th century, there was added the *steam* as the working medium and the turbines working in closed channel were constructed. The phenomenological definition as a *machine, which rotates similarly as the vortices* – from the Greek word *τυρβη = vortex* [1], opens the way to exact scientific exploration, engineering optimization and to systematic education.

There is a lot of insight obtained by experiments and numerical simulations about what happens inside the turbine. Let us mention, among others, the Ilieva's review [5], Langston's review [6], Sieverding's review [7], analysis of Denton and Pullan [8] or our own previous measurements [9], [10].

* Corresponding author: zitek@kke.zcu.cz

2 Experimental setup

2.1 VT-400 test turbine

The experimental test rig VT-400 [11] is a 1:2 scale model of a high-pressure steam turbine part. The working medium is air sucked form the atmosphere by a compressor. It is a high reaction axial single turbine stage [12]. The VT-400 test rig consists of the basic parts (see *Fig. 1*).

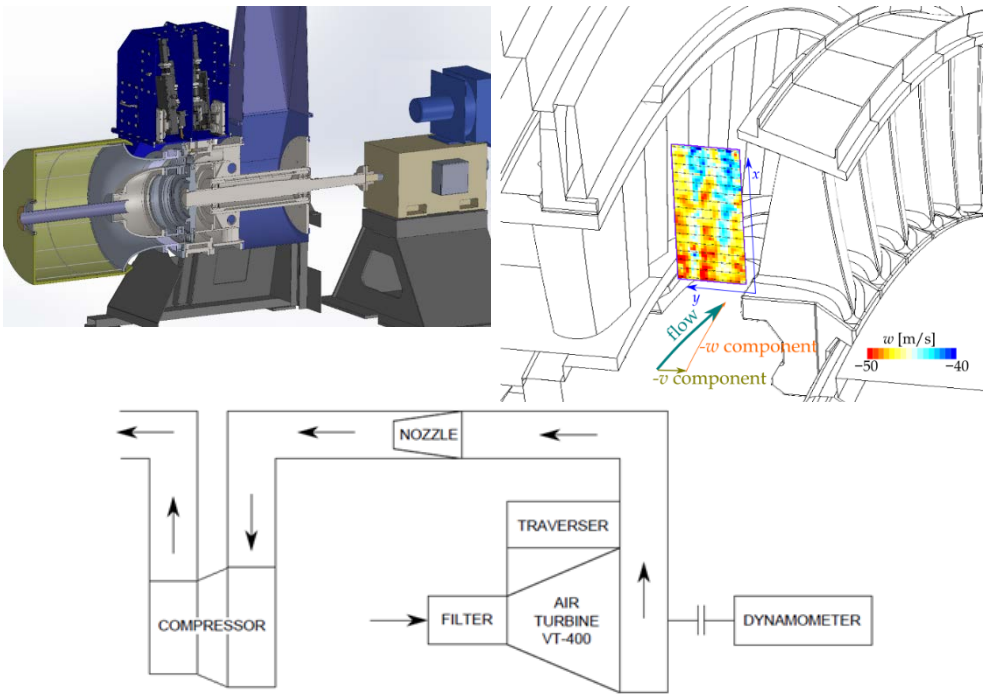

Fig. 1. Experimental VT-400 test rig (upper left) with corresponding 3D sketch of the measured PIV plane (upper right). Scheme of the entire test stand (bottom)

Some basic measuring tasks can be performed on this experimental device. The first task is the determination of the basic turbine stage characteristics, i.e. dependence of the stage efficiency on the velocity ratio $u_m/c_{02,\mathrm{is}}$ from torque measurement and static pressure taps. Parameter u_m is circumferential velocity at mid radius, and $c_{02,\mathrm{is}}$ is the isentropic velocity (see *eq. 1*).

$$c_{02,\mathrm{is}} = \sqrt{2H_{\mathrm{is}}^{ST}} \tag{1}$$

where H_{is}^{ST} is the isentropic turbine stage enthalpy drop.

The second measurement method is a detailed wake traverse measurement behind the nozzle and bucket using two 5-hole pneumatic probes. The basic parameters of the tested turbine stage are summarized in *Tab. 1*. [13]

More detailed information about the experimental device and evaluation methodology can be found in the publications [12], [11] and [13].

Tab. 1 Basic geometric parameters of tested turbine stages

Nozzle			**Bucket**		
Root diameter [mm]	D_P^{NZL}	400	Root diameter [mm]	D_P^{BCK}	400
Blade length [mm]	L^{NZL}	45.5	Blade length [mm]	L^{BCK}	47
Chord [mm]	c^{NZL}	22.5	Output rel. velocity angle [°]	β_2	14.5°
Output absolute angle [°]	α_1	14.5°			

2.2 PIV measurement system

Particle Image Velocimetry (PIV) [14] system at the University of West Bohemia (UWB) is a standard one supplied by the Dantec company. It consists of pair of FlowSense MkII cameras with resolution of 4 MPix, solid-state double pulse laser New Wave Solo with emitting energy of 0.5 J during 5 ns pulse (i.e. power during pulse is around 100 MW). The optical access for both (laser and camera) is realised through a gap for pressure probes covered by 4 mm thick desk of transparent polystyrene. The observed plane in axial × radial direction is crossed by the flow at sharp angle, thus the Stereo [14] configuration has to be used to capture the out-of-plane velocity component (see right top panel of Fig. 1). However, the Stereo configuration is much more sensitive to the calibration quality and to the homogeneity of fog as well as to the vibrations, which at the end stopped our attempts to measure even faster rotations than the mentioned 2000 RPM.

3 Results

3.1 Mean quantities

Figure 2 shows the mean vector field in the observable area. The air flows from top in the image and from behind the paper-plane. First column shows the mean vector field, where the tangential component perpendicular to the measurement plane is displayed by color. It is needed to mention, that the data are very noisy especially close to the boundary of Field of View (FoV) and at the largest probed pressure drop (bottom line in Fig. 2). It is even more apparent in the plot of turbulence intensity calculated as

$$I_T = \sqrt{\frac{\langle u^2\rangle + \langle v^2\rangle + \langle w^2\rangle - \langle u\rangle^2 - \langle v\rangle^2 - \langle w\rangle^2}{\langle u\rangle^2 + \langle v\rangle^2 + \langle w\rangle^2}} \tag{2}$$

Where $\langle\cdot\rangle$ means ensemble averaging. The large values close to the FoV boundaries are probably caused by the spurious vectors in those areas. In the central region we can observe a pair of horizontal (radial) strips of slightly higher turbulence intensity, which can be identified with the wakes past stator blades. The data at highest pressure drop are not significant.

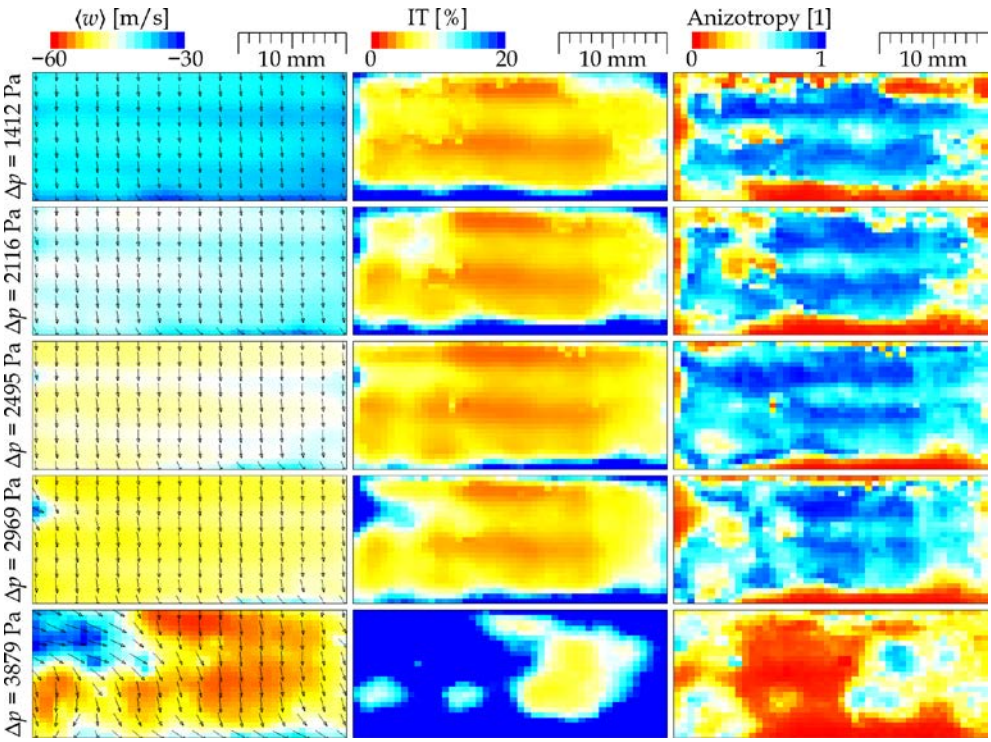

Fig. 2. Ensemble averaged field in the radial × axial plane. First column shows the mean velocity vectors only every third vector is displayed for sake of clearance; color represents velocity component (w) perpendicular to the measurement plane. Second column is the turbulence intensity showing the large amount of noise at the area borders and at the largest pressure drop. Third column shows the anisotropy of fluctuations.

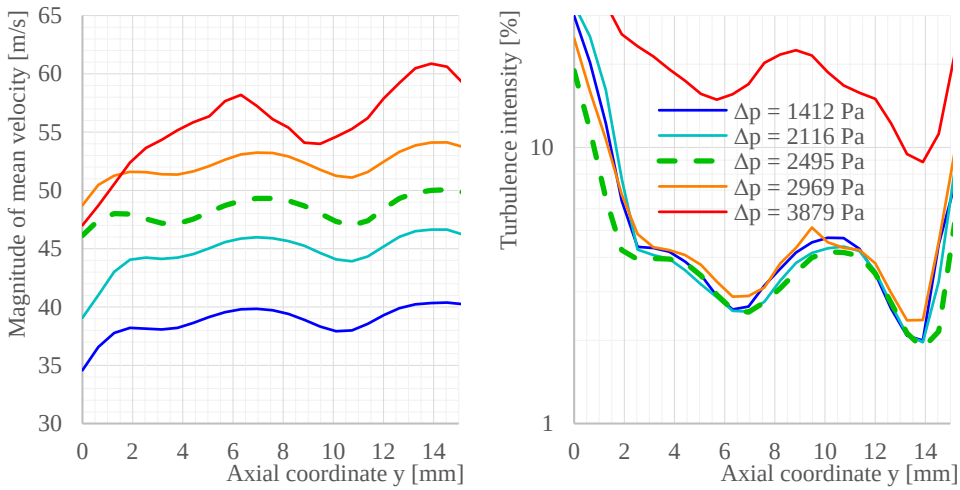

Fig. 3. Axial cut of mean velocity magnitude (left) and turbulence intensity (right). The color corresponds to pressure drop: blue for smallest, red for largest.

3.2 Anisotropy

The last column of Fig. 2 shows the anisotropy coefficient of 3D velocity fluctuations according to Lumley [15], Choi [16] and Simonsen [17], (an overview about the interpretation of the invariant of fluctuation matrix can be found in [18]). The analysis is based on the Reynolds stress tensor τ_{ij}

$$\tau_{ij} = -\rho\langle u_i' \cdot u_j' \rangle, \quad \text{where } u_i' = u_i - \langle u_i \rangle \tag{3}$$

Whose non-dimensionalised anisotropic part $b_{ij} = \tau_{ij}/\tau_{kk} - \delta_{ij}/3$ is eigen-decomposed getting three invariants, whose combination describes the level of 3D anisotropy:

$$F = 1 - \frac{9}{2} b_{ij} b_{ji} + 9 b_{ij} b_{jk} b_{ki} \tag{4}$$

A pure isotropic turbulence of Kolmogorov style [19] would display $F = 0$, however even the grid-generated turbulence [20] [21] displays a significant anisotropy [22] [23]. On the other hand, a noise might be isotropic as well (there is no reason for anisotropic behaviour). In this case, we believe, that the isotropy signal ($F \approx 0$ in Fig. 2) comes from the noise, not being a sign of ideal isotropic turbulence. The flow past an airfoil (such as turbine blade) is strongly anisotropic, as observed by other authors [24], [25] and by us as well [26] [27].

3.3 The size of fluctuation structures

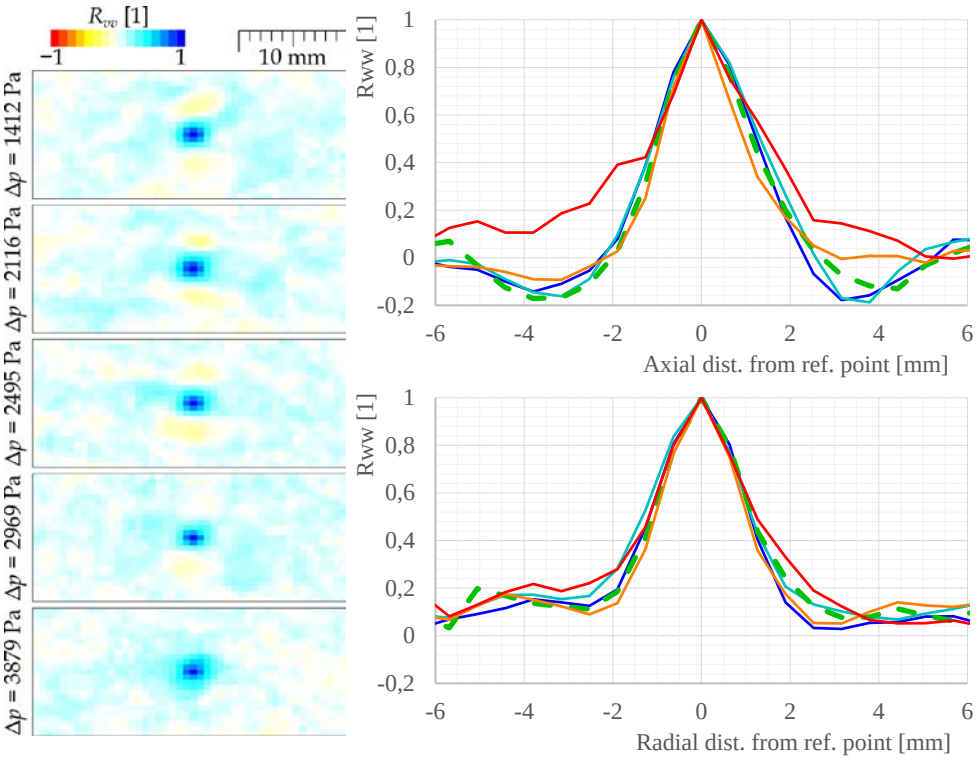

Fig. 4: Left: map of autocorrelation function of tangential velocity R_{ww} with reference point in the middle of observed area. Right: Autocorrelation as a function of axial (top) or radial (bottom) distance from reference point. The color represents the pressure drop as in Fig. 3 does.

The size of coherent structures is quantified in terms of autocorrelation function in Fig. 4. In the present case, it does not depend on the pressure drop (and thus velocity, see Fig. 3). Additionally, there is an evidence of a “wave” in axial direction caused by the structure of

alternate jet and wake past the stator wheel. On the other hand, the comparable range in radial direction suggests no two-dimensionality of the turbulence (2D turbulence would display fully correlated fluctuations along the radial coordinate).

Alternative way [19] is in the turbulence spectrum, which quantifies, how much energy is at which length-scale, standardly represented by the wave number of corresponding oscillations. We use our algorithm described in more details in [28]. The data at largest pressure drop are not valid as discussed before and again proved by the non-Kolmogorov spectrum in Fig. 5. The other data show more-or-less Kolmogorov scaling with some depletion at $k \approx 0.3\ \mathrm{mm}^{-1}$. For deeper exploration of the spectrum we would need cameras with higher resolution and better optical access into the turbine VT-400.

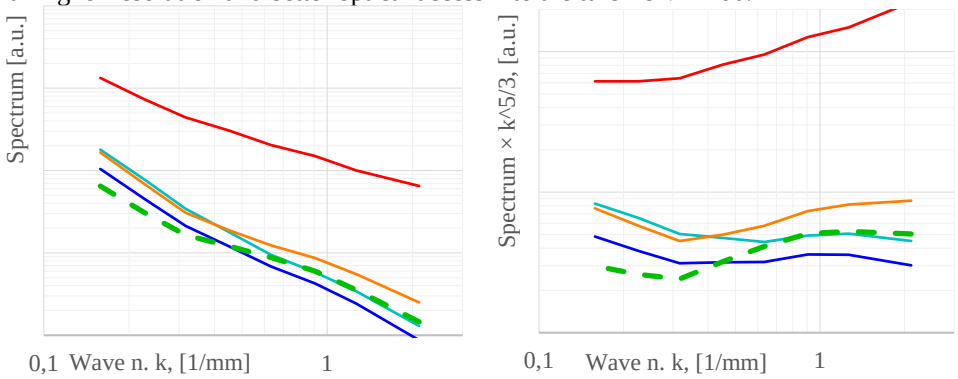

Fig. 5: Left: Power spectral density of fluctuations as a function of wave number *k*. Right: the same data as in left but multiplied by $k^{5/3}$ to highlight the differences from Kolmogorov scaling (ideal turbulence would display a horizontal line in this plot). The color represents the pressure drop same as in Fig. 3.

4 Conclusion

The possibility of PIV measurement inside the test turbine VT-400 at UWB has been proven. However, here is so many technical issues decreasing the quality and credibility of the data, that it is needed to improve our experimental setup and equipment significantly before the next measurement.

Acknowledgments

The presented work was financially supported by the TA ČR project TN01000007 and the student project SGS-2022-023 (Research and development of power machines and equipment).

References

1. C. Burdin, Annales de chimie et de physique **24**, (1824)
2. Ö. Wikander, in *Handbook of Ancient Water Technology* (Brill, Leiden, 2000), pp. 371-400
3. P. Jahren and T. Sui, *How Water Influences Our Lives* (Springer, Singapore, 2016)

4. I. Vargas and H. Gallegos, Journal of Professional Issues in Engineering **116**, (1990)
5. G. Ilieva, Defect and Diffusion Forum **379**, (2017)
6. L. Langston, Annals New Yourk Academy of Sciences **934**, (2001)
7. C. Sieverding and M. Manna, International Journal of Turbomachinery Propulsion and Power **5**, (2020)
8. J. Denton and G. Pullan, Proceedings of ASME Turbo Expo **GT2012**, (2012)
9. D. Duda, T. Jelínek, P. Milčák, M. Němec, V. Uruba, V. Yanovych and P. Žitek, International Journal of Turbomachinery Propulsion and Power **6**, (2021)
10. D. Duda, T. Jelínek, M. Němec, V. Uruba, V. Yanovych and P. Žitek, AIP Conference Proceedings **2323**, (2021)
11. M. Klimko and D. Okresa, AIP Conference Proceedings **1745**, (2016)
12. M. Klimko and D. Okresa, Acta Polytechnica **56**, (2016)
13. M. Klimko, R. Lenhard, P. Žitek and K. Kaduchová, Processes **9**, (2021)
14. C. Tropea, A. Yarin and J. Foss, *Springer Handbook of Experimental Fluid Mechanics* (Springer, Berlin, 2007)
15. J. Lumley and G. Newman, J. Fluid Mech. **82**, (1977)
16. K. Choi and J. Lumley, J. Fluid Mech. **436**, (2001)
17. A. Simonsen and P. Krogstad, Phys. Fluids **17**, (2005)
18. V. Uruba, Proceedings Topical Problems of Fluid Mechanics **2015**, (2015)
19. A. Alexakis and L. Biferale, Physics Reports **767-769**, (2018)
20. T. Kurian and J. Fransson, Fluid Dynamics Research **41**, (2009)
21. M. Mohamed and J. LaRue, J. Fluid Mech. **219**, (1990)
22. P. Roach, International Journal of Heat and Fluid Flow **8**, (1987)
23. D. Duda, V. Yanovych and V. Uruba, Processes **8**, (2021)
24. I. Solís-Gallego, A. Meana-Fernández, J. Fernández Oro, K. Argüelles Díaz and S. Velarde-Suárez, Journal of Applied Fluid Mechanics **10**, (2017)
25. G. Ozkan and H. Egitmen, Experimental Thermal and Fluid Science **134**, (2022)
26. V. Yanovych, D. Duda, V. Uruba and T. Tomášková, Processes **10**, (2022)
27. D. Duda, V. Yanovych, V. Tsymbalyuk and V. Uruba, Energies **15**, (2022)
28. D. Duda and V. Uruba, Journal of Nuclear Engineering and Radiation Science **5**, (2019)